Final Report

Development of a low-lead, high dielectric system

by

Sutin Kuharuangrong

Chulalongkorn University

Supported by: Thailand Research Fund

Under Contract No. RSA5/2539

Final Report

Development of a low-lead, high dielectric system

bу

Sutin Kuharuangrong

Chulalongkorn University

Supported by: Thailand Research Fund

Under Contract No. RSA5/2539

ACKNOWLEDGMENTS

I would like to express my sincere gratitude to Thailand Research Fund for financial support under contract no. RSA5/2539 and Chulalongkorn University throughout this work. Special thanks go to my MS students for all their help in the sample preparation and characterization. I am also indebted to Prof. Dr. Walter Schulze for his valuable advice in the resistivity measurement. Finally, I also acknowledge Dr. Chutima Eamchotchawalit and Thailand Institute of Scientific and Technological Research for their assistance for CIP and XRD measurements.

บทคัดย่อ

ในงานวิจัยนี้ได้ทำการตรวจสอบสมบัติทางไดอิเลกทริก โครงสร้าง และโครงสร้างจุลภาค ของสารบิสมัทโซเดียมไททาเนตและสารบิสมัทโซเดียมไททาเนต-เลดไททาเนตที่เติมด้วยแคทไอออน ด้วอื่นเข้าไป สมบัติทางไดอิเลกทริกถูกศึกษาเมื่อมีการเปลี่ยนแปลงอุณหภูมิและความถี่ของสารเหล่านี้ วิธีการต่างๆที่ใช้ในการคำนวนหาค่า diffuseness ที่อุณหภูมิเปลี่ยนเฟสถูกเปรียบเทียบกับผลที่ได้จาก การทดลอง สำหรับอุณหภูมิที่มีการเปลี่ยนเฟสของสารประกอบต่างๆในงานทดลองนี้ถูกกำหนดจาก ข้อมูลของค่าคงที่ไดอิเลกทริกและสัมประสิทธิการขยายตัวเมื่ออุณหภูมิเปลี่ยนไป นอกจากนี้ยังมีการ ตรวจสอบผลของแคทไอออนต่อสมบัติความต้านทานไฟฟ้าที่เปลี่ยนตามอุณหภูมิของสารเหล่านี้ด้วย

ผลการทดลองพบว่าสตรอนเทียมช่วยเพิ่มค่าคงที่ไดอิเลกทริกและลดอุณหภูมิคูรี่ ตะกั่วและ
บาเรียมเพิ่มค่าคงที่ไดอิเลกทริกที่อุณหภูมิคูรี่ ตะกั่วยังช่วยลดอัตราการเกิด aging ของสารบิสมัท
โซเดียมไททาเนต สารนี้เมื่อถูกเติมด้วยออกไซด์ของดีบุก โปแตสเซียม และในโอเบียมช่วยทำให้ค่า
คงที่ไดอิเลกทริกเปลี่ยนไปอย่างช้า ๆเมื่ออุณหภูมิเปลี่ยนไป ซึ่งเป็นสมบัติที่สำคัญของสารประเภท
relaxor แต่สารที่เติมด้วยออกไซด์ของดีบุกให้ค่าคงที่ไดอิเลกทริกต่ำเกินไปสำหรับที่จะใช้ทำเป็นตัว
เก็บประจุ ส่วนสารที่เติมด้วยออกไซด์ของโปแตสเซียมช่วยทำให้ช่วงของ antiferroelectric กว้างขึ้น
เนื่องจากอุณหภูมิเปลี่ยนเฟสที่อุณหภูมิต่ำลดลงเข้าใกล้อุณหภูมิห้อง สำหรับออกไซด์ของในโอเบียม
ลดค่าคงที่ไดอิเลกทริกของสารบิสมัทโซเดียมไททาเนต แลดไททาเนตลง ทั้งนี้เพราะปรากฎเฟสของ
โพโรคลอร์ขึ้น แคทไอออนส่วนใหญ่ที่เลือกใช้เติมเข้าไปช่วยควบคุมการโตของเกรนและปริมาณของ
แคทไอออนที่เดิมเพียงเล็กน้อยไม่ทำให้โครงสร้างเดิมของสารบิสมัทโซเดียมไททาเนต และสารบิสมัท
โซเดียมไททาเบต เลดไททาเบตเลี่ยนไป

ค่า diffuseness ที่คำนวนได้จากวิธีของ Isupov ให้ผลเหมือนกับที่ได้จากการทดลองของงาน วิจัยนี้เมื่อเทียบกับวิธีอื่น ๆ เช่น power law และ variable power law ซึ่งให้ผลที่ต่างออกไป

สำหรับค่าความด้านทานไฟฟ้าของสารบิสมัทโชเดียมไทหาเนต-เลดไททาเนตนั้นลดลงเมื่อเติม ออกไซด์ของในโอเบียม แต่ออกไซด์ของแลนทานัม และโปแตสเซียมช่วยเพิ่มค่าความด้านทานไฟฟ้า ของสารผสมนี้ ความด้านทานไฟฟ้าที่เปลี่ยนไปมากหรือน้อยขึ้นกับชนิดและปริมาณของแคทไอออน ที่เติมเข้าไปทั้งนี้ขึ้นกับ vacancies และเฟสอื่นที่เกิดขึ้นในสารประกอบ

คำหลัก สารบิสมัทโซเดียมไททาเนต-เลดไททาเนต รีแลกเซอร์ เฟอร์โรอิเลกทริก

ABSTRACT

The dielectric properties, structure and microstructure of cations modified Bi_{0.5}Na_{0.5}TiO₃ (BNT) and Pb-doped BNT ceramics were investigated in this research. The dielectric properties were studied as a function of temperature and frequency. The methods to determine the diffuseness or broadness above the Curie temperature were compared. The phase transition temperatures were obtained from the dielectric data and the coefficient of thermal expansion. In addition, the dc resistivity of this system was examined as a function of temperature.

The results show that compositions modified with strontium increase the relative dielectric permittivity and decrease the Curie temperature. Both of lead and barium can increase the maximum of dielectric permittivity. Lead also decreases the aging rate of BNT. Tin, potassium and niobium tend to give a broad dielectric constant at the transition temperature which is a characteristic of relaxor. However, the maximum dielectric permittivity of compositions with tin is too low to be useful for a capacitor. In the case of potassium, the first transition temperature moves toward lower temperature and thus, extending an antiferroelectric region. Niobium reduces the dielectric constant due to a formation of pyrochlore phase observed from the results of XRD and SEM. Most cation dopants can control the grain growth. The small amount of cations modified BNT and Pb-doped BNT does not change their structures determined from XRD.

The diffuseness calculated via Isupov's method is in agreement with the experimental results as compared to that determined from Gaussian distribution, power law and variable power law techniques.

Niobium decreases the dc resistivity of BNT-PT. With a combination of lanthanum and potassium, the resistivity of these modified BNT-PT increases. However, the type of cations and their amount affect the resistivity of BNT and BNT-PT since the vacancies and second phase take place in the compositions.

Keywords: Bi_{0.5}Na_{0.5}TiO₃-PbTiO₃, Relaxor, Ferroelectric

TABLE OF CONTENTS

LIST OF TABLES

LIST OF FIGURES

INTRODUCTION	1
PREPARATION OF CATIONS DOPED BNT-PT	2
Experimental Procedure	2
Weight loss and Microstructure analysis	
Dielectric Analysis	3
Polarization-Voltage Hysteresis	
Resistivity Measurement	4
RESULTS AND DISCUSSION	5
SUMMARY AND CONCLUSIONS	35
REFERENCES	37
APPENDIX A: Oxides and Carbonates Used in Synthesis	39
APPENDIX B: Isupov's model	40
PUBLICATIONS	42

LIST OF TABLES

1.	The calculated lattice parameter and x-ray density	
	for some compositions	9
2.	Average %weight loss and grain size versus composition	
	sintered at 1175 °C	9
3.	Maximum K', the first and second transition temperatures	
	as a function of frequency and composition	23
4.	Power n and diffuseness parameter, δ , calculated from	
	the variable power equation for Pb-doped BNT	25
5.	The diffuseness, δ , and the Curie constant, C,	
	calculated from Isupov's model for Pb-doped BNT	26
6.	Activation energy calculated in the range of	
	250 °C to 400 °C of some compositions	34

LIST OF FIGURES

1.	DTA traces of the mixed raw materials for lanthanum, magnesium	
	and niobium-doped BNT-PT	6
2.	DTA traces of the mixed raw materials for zirconium and	
	zinc-niobium doped BNT-PT	7
3.	XRD patterns of (a). 0.9Bi _{0.48} La _{0.02} Na _{0.48} K _{0.02} TiO ₃ -0.1PT,	
	(b). 5%Nb-doped BNT-10PT, (c). 10%Nb-doped BNT-10PT	
	(d). 5%Nb-doped BNT-15PT	8
4.	SEM photomicrograph of 5%La-doped 0.9BNT-0.1PT	
	sintered at 1175 °C	10
5.	SEM photomicrograph of 0.9Bi _{0.48} La _{0.02} Na _{0.48} K _{0.02} TiO ₃ -0.1PT	
	sintered at 1175 °C	10
6.	SEM photomicrograph of 0.9Bi _{0.48} La _{0.02} Na _{0.46} K _{0.04} TiO ₃ -0.1PT	
	sintered at 1175 °C	11
7.	SEM photomicrograph of 5%Nb-doped BNT-10PT	11
8.	SEM photomicrograph of 5%Nb-doped BNT-15PT	12
9.	SEM photomicrographs of 10%Nb-doped BNT-10PT	
	(a). from mixed all raw materials (b). from precursor	13
10.	SEM photomicrograph of 0.9BNT-0.1PbTi _{0.9} Mn _{0.1} O ₃	14
11.	Change in relative permittivity and dissipation factor with	
	temperature and frequency of 0.9(Bi _{0.45} La _{0.05} Na _{0.5} TiO ₃)-0.1PT	15
12.	Change in relative permittivity and dissipation factor with	
	temperature and frequency of 0.88(Bi _{0.48} La _{0.02} Na _{0.5} TiO ₃)-0.12PT	16
13.	Change in relative permittivity and dissipation factor with	
	temperature and frequency of 0.9(Bi _{0.48} La _{0.02} Na _{0.48} K _{0.02} TiO ₃)-0.1PT	17
14.	Change in relative permittivity and dissipation factor with	
	temperature and frequency of 0.9(Bi _{0.48} La _{0.02} Na _{0.46} K _{0.04} TiO ₃)-0.1PT	18
15.	Change in relative permittivity and dissipation factor with	
	temperature and frequency of 5%Nb-doped BNT-10PT	19
16.	Change in relative permittivity and dissipation factor with	
	temperature and frequency of 5%Nb-doped BNT-15PT	20
17.	Change in relative permittivity and dissipation factor with	
	temperature and frequency of 10%Nb-doped BNT-10PT	21
18.	Change in relative permittivity and dissipation factor with	
	temperature and frequency of 0.9BNT-0.1PbTi _{0.9} Mn _{0.1} O ₃	22

19.	Dependency of the reciprocal dielectric permittivity on (T-Tm) ²	
	for Pb-doped BNT	26
20.	Dependency of the reciprocal dielectric permittivity on (T-Tm) ^{1.4}	
	for BNT	27
21.	Dependency of the reciprocal dielectric permittivity on (T-Tm) ^{1.9}	
	for Pb-doped BNT	27
22.	Comparison of the experimental dielectric results and the	
	calculation from Isupov's model for Pb-doped BNT	28
23.	Polarization-Voltage hysteresis loop for 0.9(Bi _{0.48} La _{0.02} Na _{0.48} K _{0.02} TiO ₃)	
	-0.1PT with a maximum voltage at 4 kV	29
24.	Polarization-Voltage hysteresis loop for 0.9(Bi _{0.48} La _{0.02} Na _{0.46} K _{0.04} TiO ₃)	
	-0.1PT with a maximum voltage at 4 kV	29
25.	Polarization-Voltage hysteresis loop for 5%Nb-doped BNT-15PT	
	with a maximum voltage at 4 kV	30
26.	Polarization-Voltage hysteresis loop for 10%Nb-doped BNT-10PT	
	with a maximum voltage at 4 kV	30
27.	Resistivity versus 1000/T of (a). $0.9(Bi_{0.48}La_{0.02}Na_{0.48}K_{0.02}TiO_3)-0.1PT$	
	(b). 0.9(Bi _{0.48} La _{0.02} Na _{0.46} K _{0.04} TiO ₃)-0.1PT measured with	
	an applied voltage of 500 volts	31
28.	Linear equation obtained from a curve fitting of	
	(a). 0.9(Bi _{0.48} La _{0.02} Na _{0.48} K _{0.02} TiO ₃)-0.1PT	
	(b). 0.9(Bi _{0.48} La _{0.02} Na _{0.46} K _{0.04} TiO ₃)-0.1PT	32
29.	Resistivity versus 1000/T of Nb-doped BNT-PT measured	
	with an applied voltage of 500 volts	33
30.	Linear equation obtained from a curve fitting of 5%	
	and 10%Nb-doped BNT-PT	33
31.	Linear equation obtained from a curve fitting of 5%Nb-doped	
	BNT-15PT in the ranges of 280-350 °C and 350-400 °C	34

Introduction

Bi_{0.5}Na_{0.5}TiO₃ (BNT) was first synthesized by G.A. Smolenskii and A.I. Agranovskaya¹ in 1959. A few years later² it was found to be ferroelectric from the polarization-electric field hysteresis loops and its lattice constant determined by assuming a cubic structure was 3.88 angstrom. In 1974 K. Sakata et. al.³ studied an additional phase transition of BNT ceramics from ferroelectric to antiferroelectric at 220 °C since this transition temperature moved toward higher temperature with an applied dc field. However, the optical and x-ray investigations^{3,4} did not show any structural changes from the antiferroelectric to the ferroelectric phase.

The phase transitions of BNT were also studied from the K'(T) curve. There were obviously two phase transitions^{2-3,5-6} on the K'(T) curve, a hump around 220 °C and a maximum of K' around 325-335 °C. Studies on the dielectric properties as a function of temperature^{2,5-7} have shown that BNT generally exhibits a broad maximum in the dielectric constant or a diffuse phase transition. The maximum K' at 10 kHz was 2600 around 335 °C⁶ and the dielectric loss increased rapidly above this temperature.

After 1989 the experimental investigations of BNT were mostly related to the modifications concerning piezoelectric⁸-11 and pyroelectric⁸ properties. BNT doped with 6.5% of strontium and 6.5% of lead was studied for ultrasonic transducers⁸,10 at high frequency. Doped with 5% of strontium and 5% of lead this composition was considered to be useful for pyroelectric sensors as compared to lead-zirconate-titanate (PZT). Although lead improved the properties of BNT, many studies have been performed on the lead-free BNT. The compositional modifications of BNT-PT as a candidate material for a high temperature capacitor dielectric, however, have not been investigated.

In this research the experiments would consider the effect of dopants on the dielectric constant and the transition temperatures. In order to be useful in developing a high temperature dielectric, the objective of this research would concentrate on the dielectric peak of the transition temperature. It was expected to shift into the working temperature region and distribute the transition peaks so that the dielectric constant related to temperature was high and broad. In addition, the diffuseness or broadness representing the distribution of the polar phase in the nonpolar phase above the Curie temperature would be determined. The following methods such as Gaussian distribution, power law, variable-power law and Isupov's model, would be used to calculate the diffuseness of BNT-PT and compared to the results from the experiments. Moreover, the effects of modifiers on the structure, microstructure and resistivity were examined.

Preparation of cations doped BNT-PT

BNT is ferroelectric at room temperature and has the perovskite structure with a general formula ABO₃, where A and B are cations. For BNT two types of ions, Bi and Na, are in the A sites and Ti is in the B site.

Earlier investigators prepared BNT ceramics by a conventional technique. Reagent grades⁸ or pure grades of Bi₂O₃, Na₂CO₃ and TiO₂ were used as the starting materials and mixed in a stoichiometric ratio. The milled powder was calcined at 750-800 °C for one hour. After calcining, the ground and milled powder was pressed into a disk and sintered at 1080-1100 °C for two hours. Isupov et. al.¹² compared two methods of preparation for Bi_{0.5}Na_{0.5}TiO₃-PbTiO₃ solid solution. He made this solid solution directly from oxides and carbonates. In the other method, he first prepared the perovskites and combined the synthesized titanates.

In this research, the solid solution was prepared from mixing all oxides and carbonates raw materials.

Experimental Procedure

All compositions for this research were prepared according to the conventional ceramic technique of mixing and calcining all oxides and carbonates. Reagent grades of oxides and carbonates as listed in Appendix A were used as the starting raw materials. They were weighed and mixed by ball-milling for 5-6 hours in high density polyethylene bottles using zirconia rods and ethanol. After drying, the mixture was calcined in oxygen with a heating rate of 2 °C/min, and held at the reaction temperatures. The reaction temperatures were determined from the differential thermal analyzer^a. The data were taken with a heating rate of 10 °C/min in oxygen. The correction of a baseline was obtained during or after the measurement. Although the fast heating rate of 10 °C/min was used, the actual heating rate for calcining was only 2 °C/min to complete all the reactions of a large amount of powder.

After calcining, the powder was taken to characterize a phase from x-ray diffractometer^b. The machine used Cu Kα radiation. The voltage was 40 kV and the current was 30 mA. The data were collected from 20-60 degree two-theta. Silicon powder was used as an internal standard.

^a Perkin-Elmer DTA7, USA

b Shimadzu XRD-6000, Japan

The calcined material was remilled and polyvinyl alcohol was added as a binder in the last hour of milling. The slurry was dried and then ground in an agate mortar to -150 micron. The powder was pressed into disks on a single action dry-press with a pressure of 30 MPa and then followed by cold-isostatic press with a pressure of 190 MPa.

After binder burn-out with a heating rate of 1 °C/min and 75 min hold at 540-550 °C in oxygen, the disks were weighed to determine the weight before sintering. Then, the disk was placed on Pt-foil in a closed crucible with no packing powder and sintered with a heating rate of 4 °C/min and an hour soaking period at the maximum of sintering temperature. The sintered samples were cooled in the furnace.

Weight loss and Microstructure analysis

The weight loss was measured from the weights before and after sintering which were determined to $\pm\,0.01$ mg. The microstructure of the samples was observed from the scanning electron microscope^c. The samples were polished and thermally etched. The average grain sizes were determined from micrographs using the line intercept method.

Dielectric Analysis

The diameter and thickness of disks were measured with verneir calipers for the calculation of the relative permittivity (K'). The disks were electroded with silver paste by painting. After firing at 710 °C, the sample was put on the sample holder, which was inside a tube furnace^d. All capacitance and dissipation factor measurements were obtained from Impedance Analyzer^e using a 4 terminal configuration. All data were collected every 2 or 3 °C with increasing temperature at 3 °C/min from room temperature to 400 °C. In addition, they were measured at different frequencies, 1, 10, 100 kHz and 1 MHz, respectively. The relative permittivity was calculated from the capacitance and its dimension.

$$C = \frac{\mathcal{E}_0}{d} K' A$$

where C is the capacitance (Farad);

 ε_{o} is the permittivity of free space (8.85 x 10⁻¹⁴ F/cm);

A is an area of the electrode (cm²) and

d is the distance between electrode or thickness of the sample (cm)

^c JEOL JSM-5410LV, Japan

d Carbolite Tube Furnace Model STF15/75/450, England

e Yokogawa HP4192A Impedance Analyzer, Japan

The diffuseness of some compositions was determined by using Isupov's model¹³. The method for calculating all the parameters was given in Appendix B.

Polarization-Voltage Hysteresis

The test samples were electroded with silver paste and fired at 710 °C. Polarizations of the samples were measured on a virtual ground mode^f with an applied maximum voltage of 4 kV. The samples were held in an insulating oil bath during measurement.

Resistivity Measurement

After the capacitance measurements, the resistances of the samples were collected every 5 °C with an increasing temperature from room temperature to 400 °C. All data were obtained from Megohmmeter^g with an applied dc field of 500 volts. The measurement technique is that of applying a constant dc voltage to the sample and measuring the resistance as it reaches the desired temperature. The resistivity can be calculated from the following equation.

$$R = \rho \frac{1}{A}$$

where R is the resistance in ohm;

ρ is the resistivity in ohm-cm;

l is the length of sample or the distance between electrode in cm;

A is an area of electrode in cm²

f RT6000HVS, Radiant Technologies, Inc., USA

g AMPROBE Model No. AMB-5 kV, $50k\Omega$ - $50G\Omega$, USA

Results and Discussion

Figures 1 and 2 show DTA traces of the milled raw materials of the compositions of cations doped BNT-PT. The results in Figure 1 indicate that the reactions of lanthanum, magnesium and niobium-doped BNT-PT complete before 750 °C. However, with zirconium the reaction completes at higher than 750 °C, and doped with zirconiobium it completes at 1000 °C or higher as illustrated in Figure 2. During calcination soaking for 90 min at the reaction temperatures, particularly at 320-330 °C and at maximum calcining temperature, is used throughout this research. The suitable calcining schedule for each composition is determined from the result of DTA. It should be noted here that the compositions with zinc have a high loss during calcination. Moreover, most of them crack after forming the pellets.

Figure 3 illustrates the XRD patterns at room temperature which show a perovskite phase for the calcined materials. There is a small hump observed at two-theta around 30 degree and can be seen clearly as the amount of niobium is increased as shown in 10% of niobium doped BNT-10PT. This may be due to an existence of a pyrochlore phase in this solid solution. This phase always exhibits with a perovskite material since it is an intermediate phase before transforming to a perovskite phase. The real structure of this phase in this compound is still incomprehensive since it has not been documented in the literature before. Furthermore, it is hard to synthesize a pure phase. In general, the presence of excess or deficient of PbO affects the formation of the pyrochlore phase.

The results from Figure 3 indicate that all compositions of BNT-PT solid solution with a small amount of dopants have the same structure. This assumption is obtained although there is a limitation of XRD resolution. The lattice parameter at room temperature of those materials was determined by a cubic approximation. This may be done because the angular of the pseudocubic distortion is too small and the structural angle is close to 90°. The calculated lattice parameter is also given in Table 1.

From Table 1 a lattice constant is an average value calculated from 100, 110 and 200 peaks. Although there is possibly systematic error from the goniometer, it is not corrected here since this is not allowed to calibrate from the instrument owner. This error appears on the located peaks of silicon powder used as an internal standard.

The results from Table 1 show that strontium substituted bismuth and sodium in the A-site can increase a lattice constant of BNT. This may be because the size of

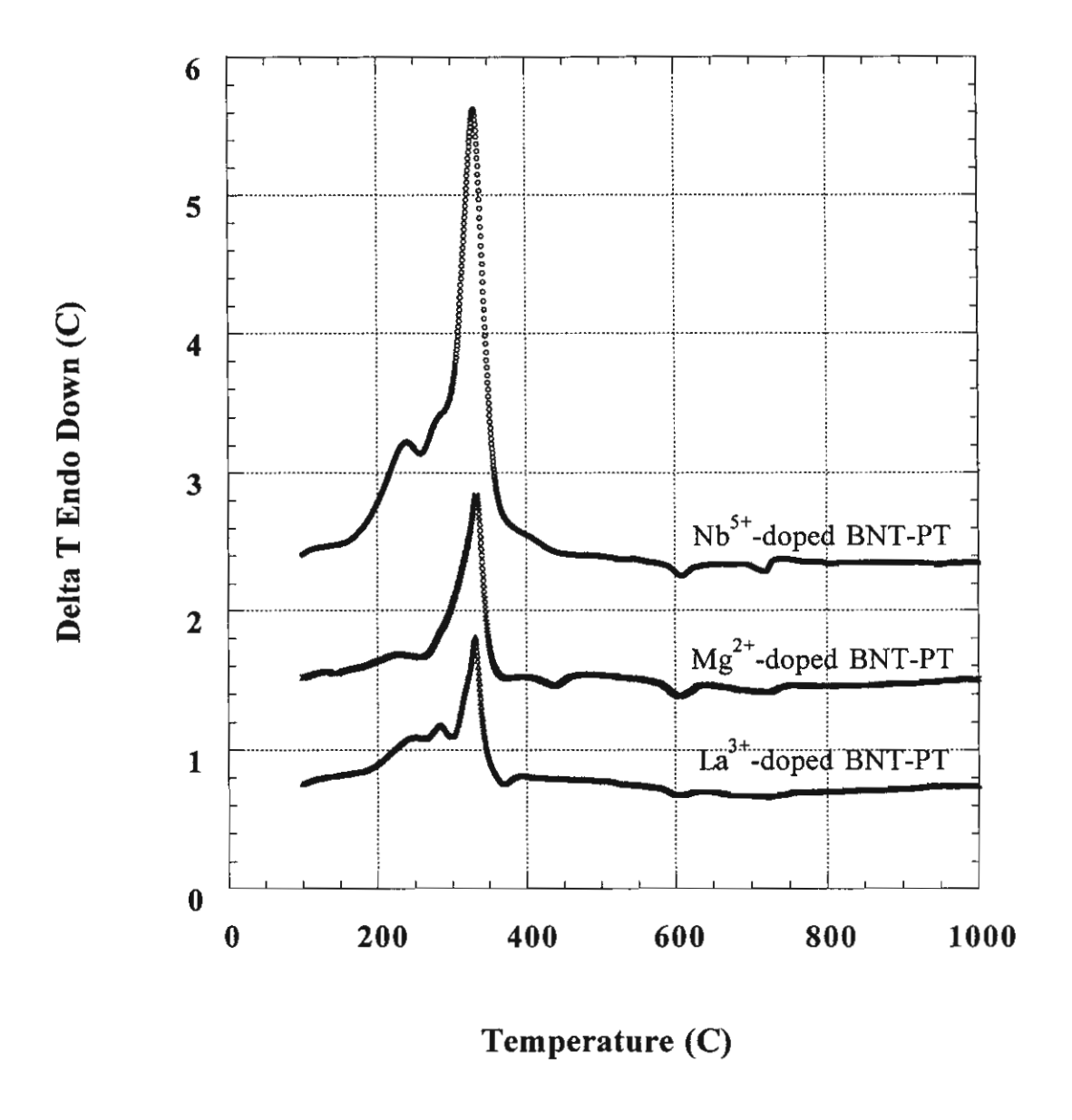


Figure 1 DTA traces of the mixed raw materials for lanthanum, magnesium and niobium-doped BNT-PT

strontium ion is larger than an average size of both bismuth and sodium ions. Like strontium, lead increases the lattice constant of this solid solution since the ionic radius of lead is larger than that of bismuth and sodium. A similar effect is shown in 5%Nb-doped BNT-10PT as compared to that of 5%Nb-doped BNT-15PT. Although the size of niobium is larger than that of titanium, the lattice parameter of 5%Nb-doped BNT-10PT increases in little compared to that of 10%Nb-doped BNT-10PT. This is probably due to a larger amount of bismuth content in 5%Nb-doped than in 10%Nb-doped BNT-10PT.

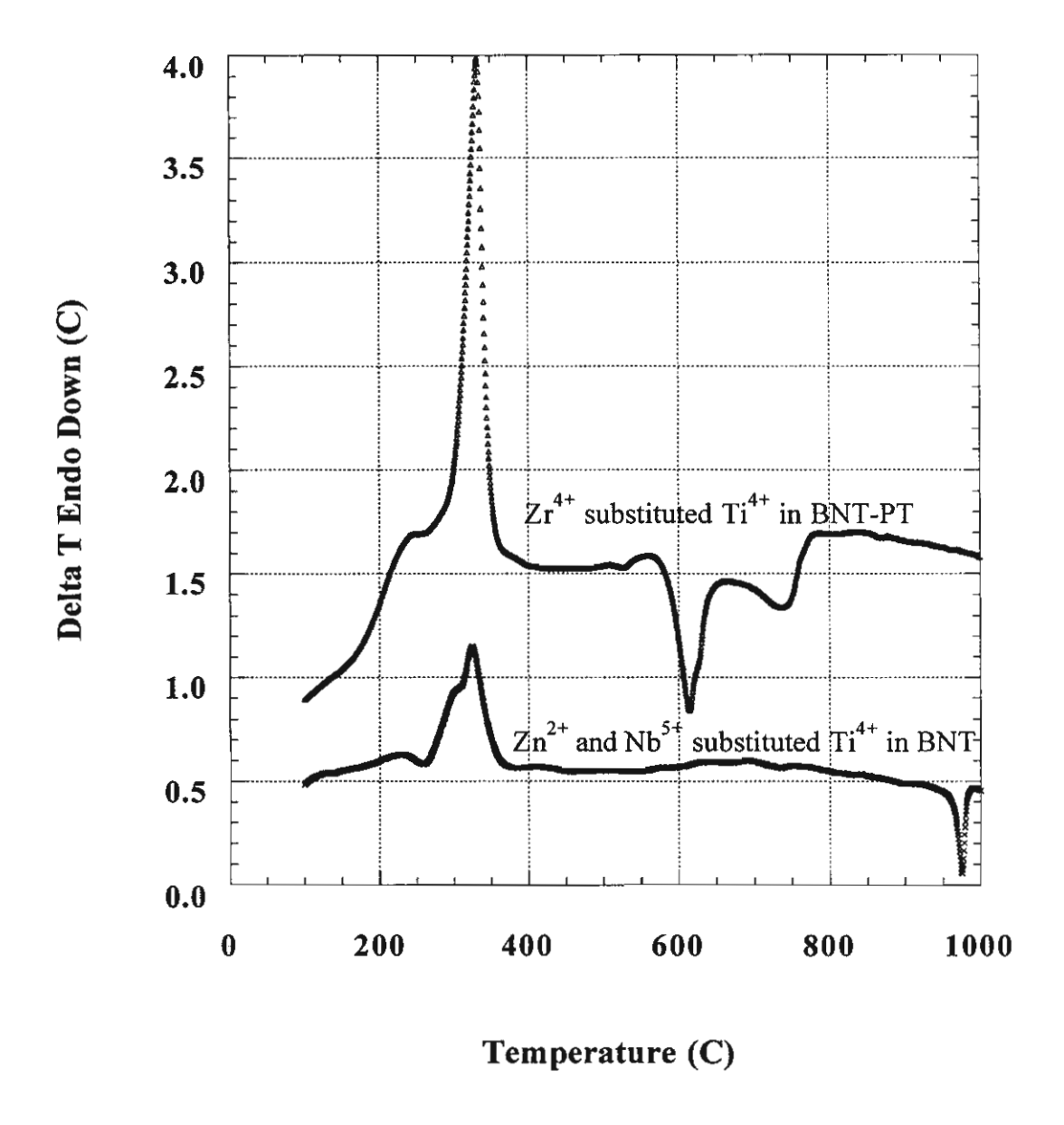


Figure 2 DTA traces of the mixed raw materials for zirconium and zinc-niobium doped BNT-PT

The weight loss and average grain size of some compositions are summarized in Table 2. The weight loss of those compositions was determined after sintering at 1175 °C. The results show that an increase amount of lead also increases the weight loss due to evaporation of lead during sintering. With lanthanum and potassium dopants the weight loss of BNT-10PT increases. From these results, an additional one percent each of lead oxide and lanthanum oxide as starting materials is necessary during preparation.

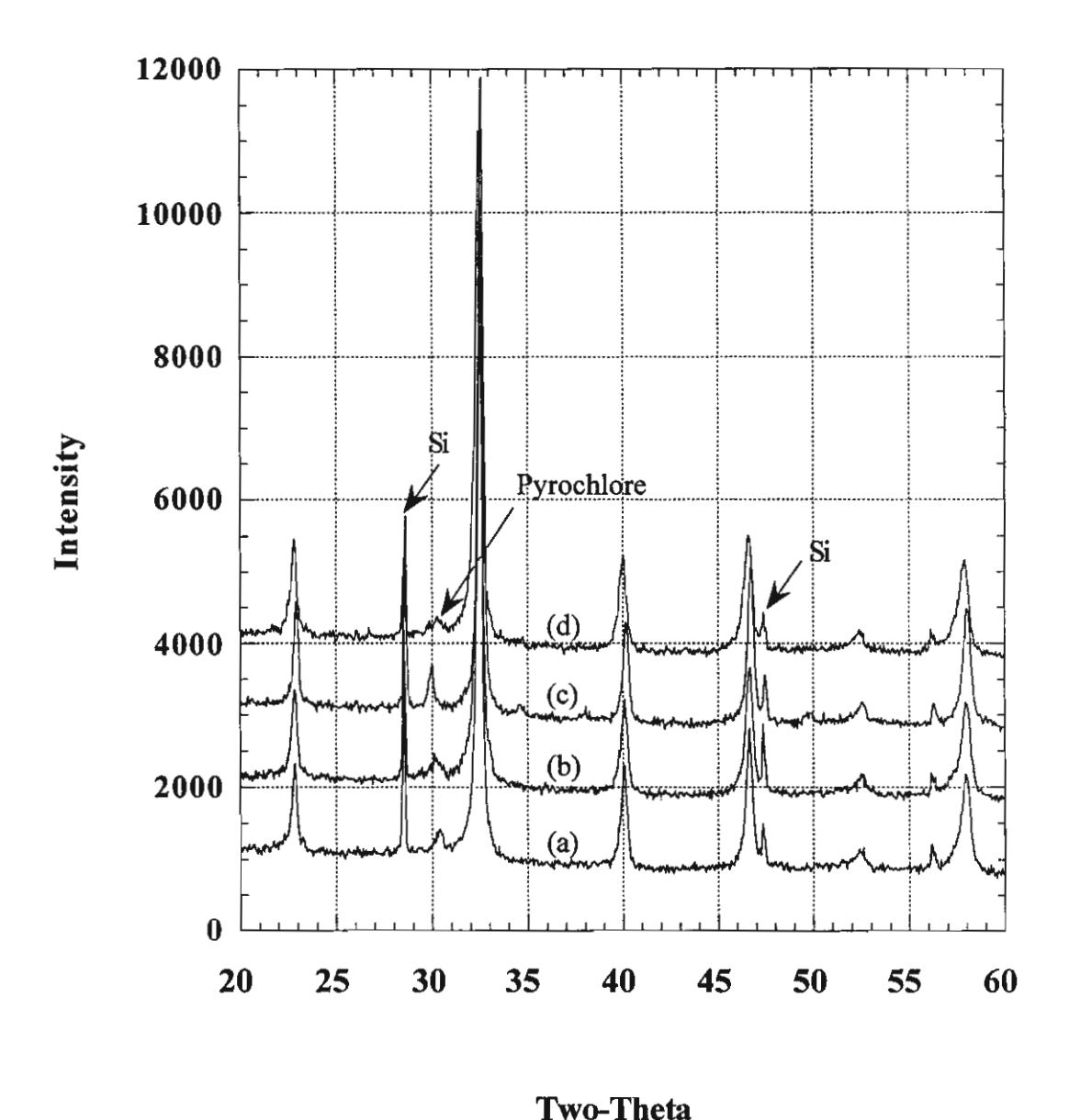


Figure 3 XRD patterns of (a). 0.9Bi_{0.48}La_{0.02}Na_{0.48}K_{0.02}TiO₃-0.1PT, (b). 5%Nb-doped BNT-10PT, (c). 10%Nb-doped BNT-10PT, (d). 5%Nb-doped BNT-15PT

A similar result is also shown in the compositions with a higher sodium content. With some extent of other dopants such as manganese, aluminum and iron, the weight loss does not change much from a base material. In contrast, zirconium or tin substituted entire titanium drastically increases the weight loss. This may imply that zirconium and tin ions could not form a suitable compound with bismuth-sodium.

Table 1 The calculated lattice parameter and x-ray density for some compositions

Composition	Lattice constant (A)	X-ray density (g/cc)
95BNT-5SrT	3.8834	5.97
90BNT-10SrT	3.8863	5.92
95(BN5PT)-5SrT	3.8924	6.05
95(BN10PT)-5SrT	3.8976	6.15
5%Nb-doped BNT-10PT	3.8978	6.13
5%Nb-doped BNT-15PT	3.9016	6.24
10%Nb-doped BNT-10PT	3.8973	6.07
0.9Bi _{0.48} La _{0.02} Na _{0.48} K _{0.02} TiO ₃ -0.1PT	3.8944	6.19

BNT=Bi_{0.5}Na_{0.5}TiO₃ SrT=SrTiO₃ PT=PbTiO₃

Table 2 Average %weight loss and grain size versus composition sintered at 1175 °C

Composition	%weight loss	average grain size (µm)
0.9Bi _{0.48} La _{0.02} Na _{0.48} K _{0.02} TiO ₃ -0.1PT	1.08	2-3
0.9Bi _{0.48} La _{0.02} Na _{0.46} K _{0.04} TiO ₃ -0.1PT	0.95	long grains
0.9BNT-0.1PbTi _{0.9} Mn _{0.1} O ₃	0.70	6-8
5%Nb-doped BNT-10PT	0.82	2.5-3.0
5%Nb-doped BNT-15PT	0.99	1.5-2.5
10%Nb-doped BNT-10PT	0.68	4-5/2-3*

BNT=Bi_{0.5}Na_{0.5}TiO₃

PT=PbTiO3

Figures 4-10 show SEM photomicrographs of the polished samples of some compositions sintered at 1175 °C. Lanthanum decreases the grain size of BNT-PT as displayed in Figure 4. The amount of potassium dopant affects the grain shape of BNT-10PT. Potassium substituted into sodium-site of BNT-PT gives long grains as appeared in Figure 6. Only small amount of potassium (Figure 5) can maintain a grain shape of BNT-PT although some grains tend to be elongate.

^{*4-5} μm prepared from mixing all raw materials, 2-3 μm prepared from precursor

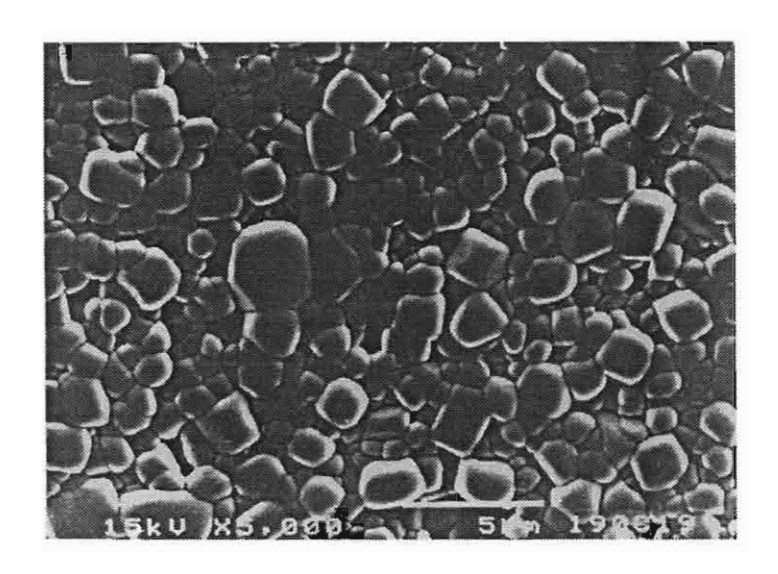


Figure 4 SEM photomicrograph of 5%La-doped 0.9BNT-0.1PT sintered at 1175 °C

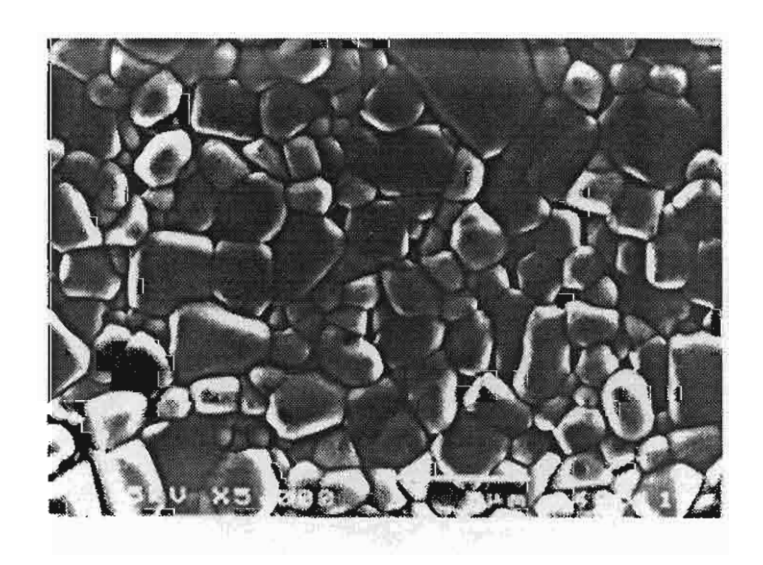


Figure 5 SEM photomicrograph of 0.9Bi_{0.48}La_{0.02}Na_{0.48}K_{0.02}TiO₃-0.1PT sintered at 1175 °C

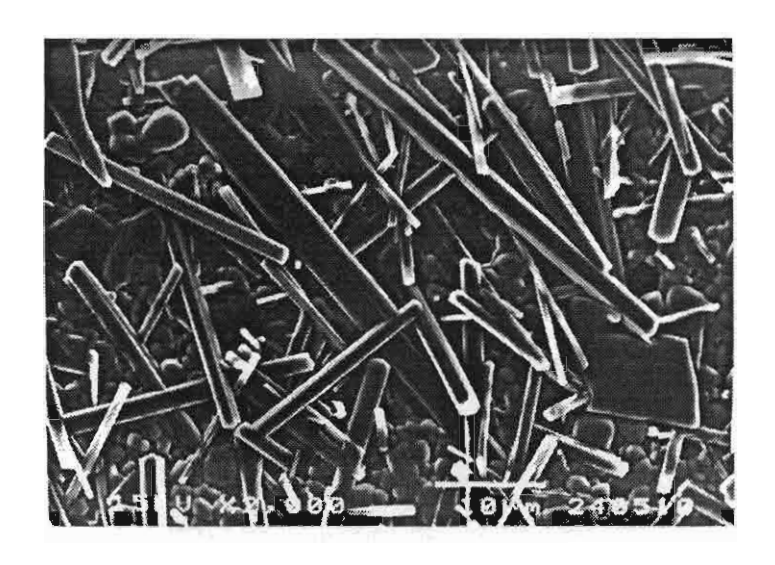


Figure 6 SEM photomicrograph of 0.9Bi_{0.48}La_{0.02}Na_{0.46}K_{0.04}TiO₃-0.1PT sintered at 1175 °C

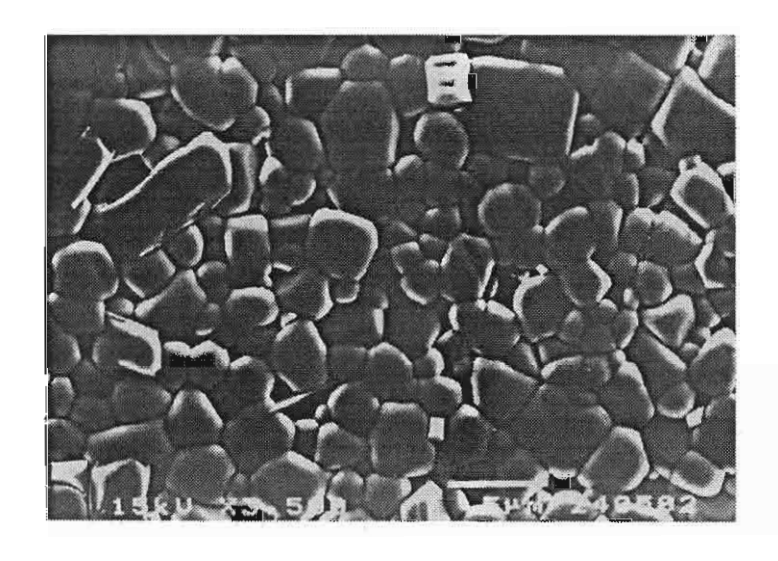


Figure 7 SEM photomicrograph of 5%Nb-doped BNT-10PT

Niobium influences the formation of pyrochlore phase represented in white grains as shown in Figures 7-9. This may support the result of XRD peak observed at two-theta of 30 degree, exhibiting an existence of a pyrochlore phase. Preparation via precursor method possibly reduces not only this phase but the grain size. In contrast to the result obtained from La-doped 0.9BNT-0.1PT, manganese increases the grain size as seen in Figure 10 although the distribution of small grains is throughout the sample. The average grain size of some compositions is also given in Table 2.

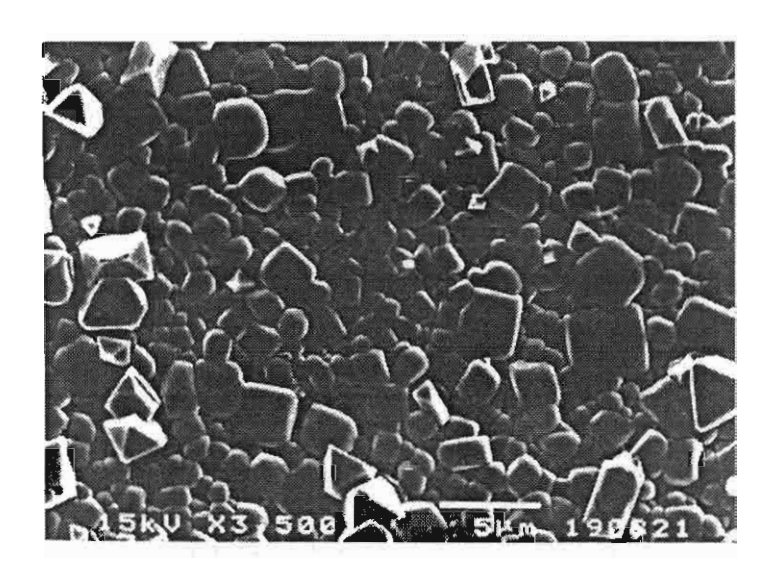
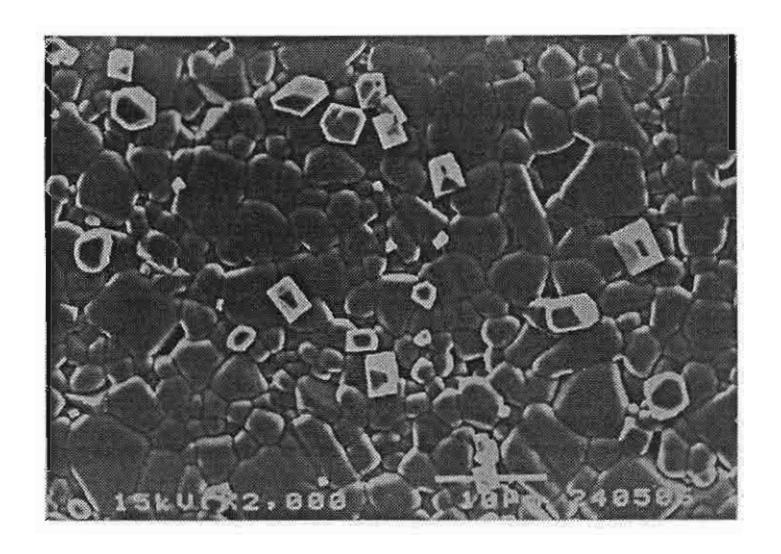
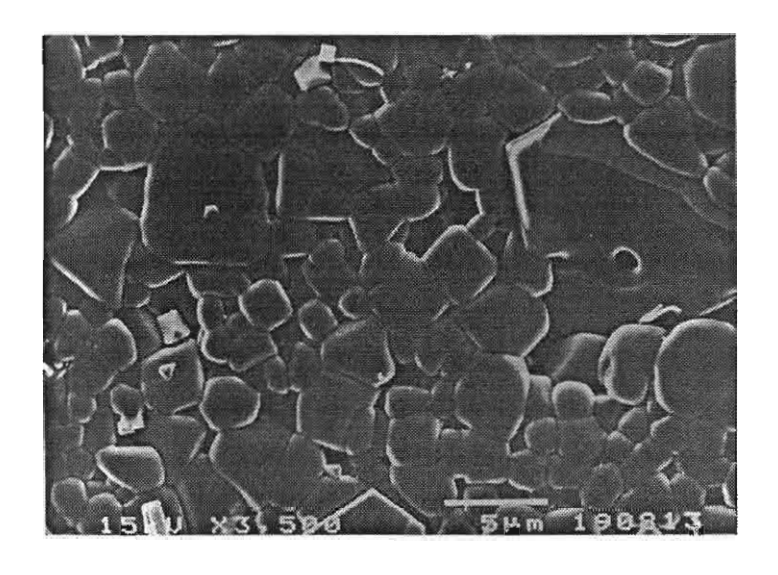


Figure 8 SEM photomicrograph of 5%Nb-doped BNT-15PT

Figures 11-17 show the results of relative permittivity, so called dielectric constant (K'), and dissipation factor of some compositions as a function of temperature and frequency. Figures 11 and 12 show the effect of lead and lanthanum on the dielectric properties of BNT. Lead increases the dielectric constant throughout the measurement temperatures. Lanthanum decreases not only the dissipation factor but the Curie point determined from the temperature at the maximum value of dielectric constant. Figures 13 and 14 show that potassium can extend an antiferroelectric region of BNT-PT, giving the first transition down toward 60 °C as appeared in the results of dielectric constant and dissipation factor. The maximum of dissipation factor around 75 °C at 1 kHz of 0.9Bi_{0.48}La_{0.02}Na_{0.48}K_{0.02}TiO₃-0.1PT in Figure 13 indicates the first transition temperature. It is observed with increasing temperatures at higher frequencies, i.e 80 °C at 100 kHz and 90 °C at 1 MHz, which is a characteristic of a relaxor. An increase in the amount of potassium tends to lower the first transition temperature to the room temperature and increase the Curie point as shown in Figure 14. The dielectric constant in the antiferroelectric range and at the Curie temperature also decreases.



(a) X 2000



(b) X 3500

Figure 9 SEM photomicrographs of 10%Nb-doped BNT-10PT (a). prepared from mixing all raw materials

(b). prepared from precursor

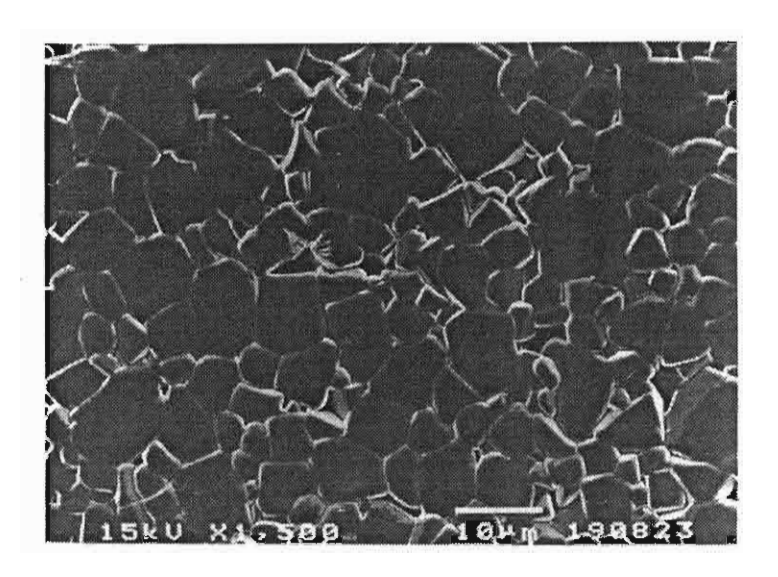
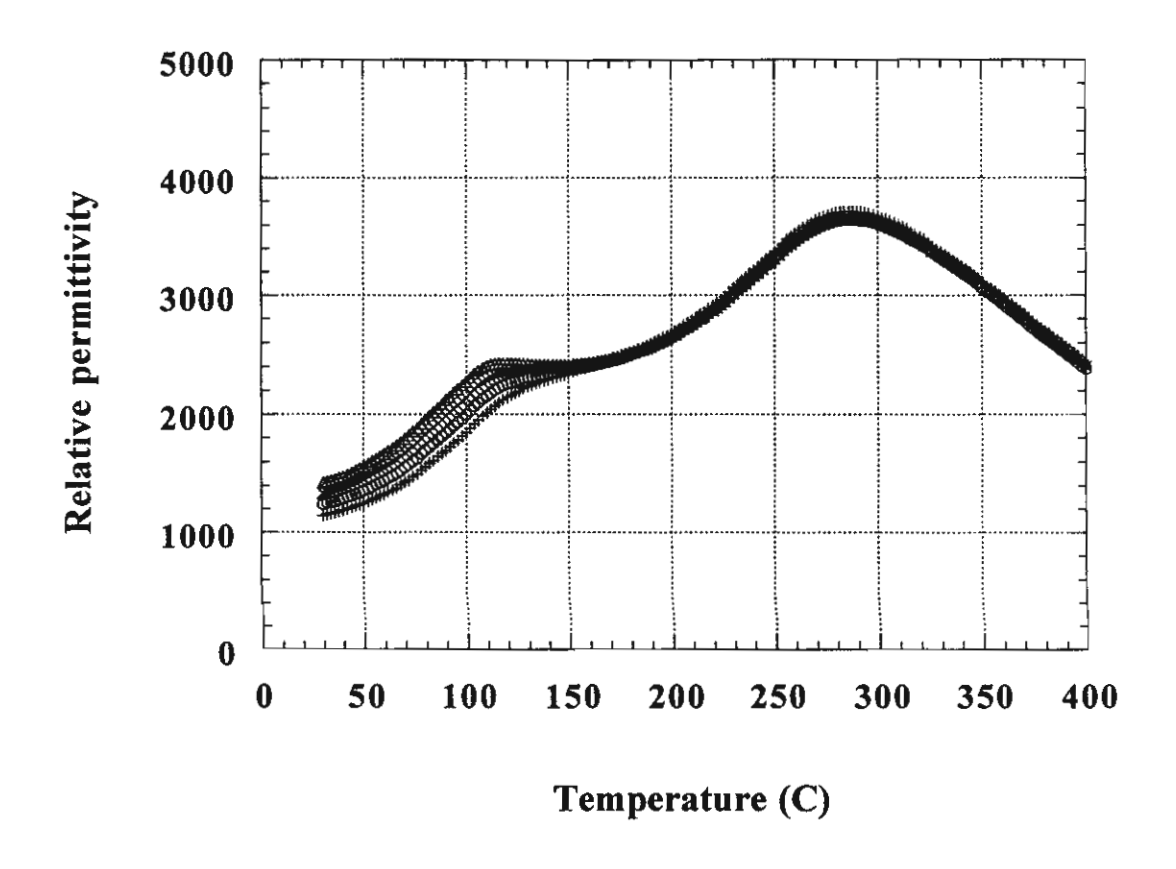


Figure 10 SEM photomicrograph of 0.9BNT-0.1PbTi_{0.9}Mn_{0.1}O₃

From the results in Figures 15-17, niobium diminishes the maximum dielectric constant and the Curie temperature. The results of dielectric constant of 5% and 10% of niobium doped BNT-PT show that these compositions should be good candidate materials for a high temperature relaxor. These materials should be further study for applications. In contrast to niobium, lead increases the maximum dielectric constant and the Curie point as illustrated in Figure 16.

Figure 18 shows the effect of manganese on the dielectric properties of BNT-10PT. Manganese lowers the dielectric constant at room temperature. In addition, it reduces a range of antiferroelectric region and has a sharp rise of the dielectric constant at 180 °C, suggesting a more ordered structure. Although manganese used in BaTiO₃ decreases the dielectric loss, in BNT-10PT the dissipation factor of this solid solution is higher, especially at low frequency.



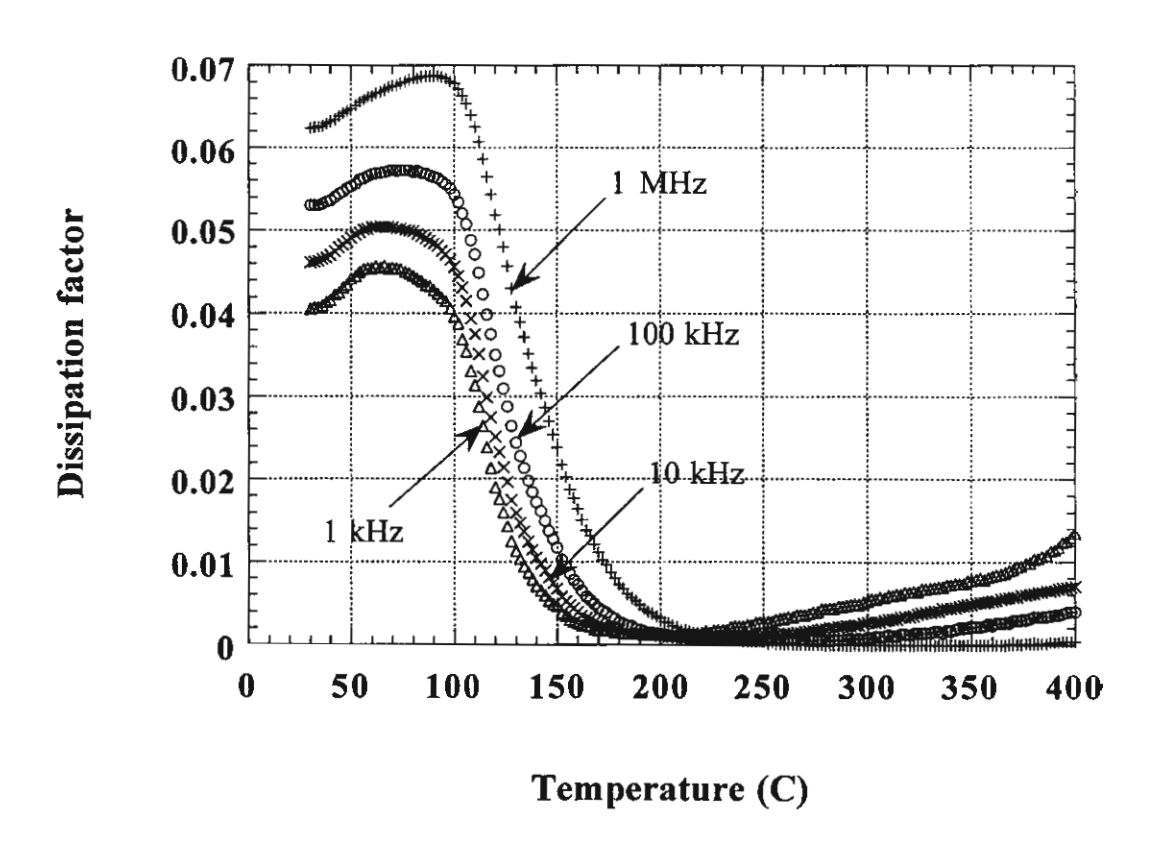
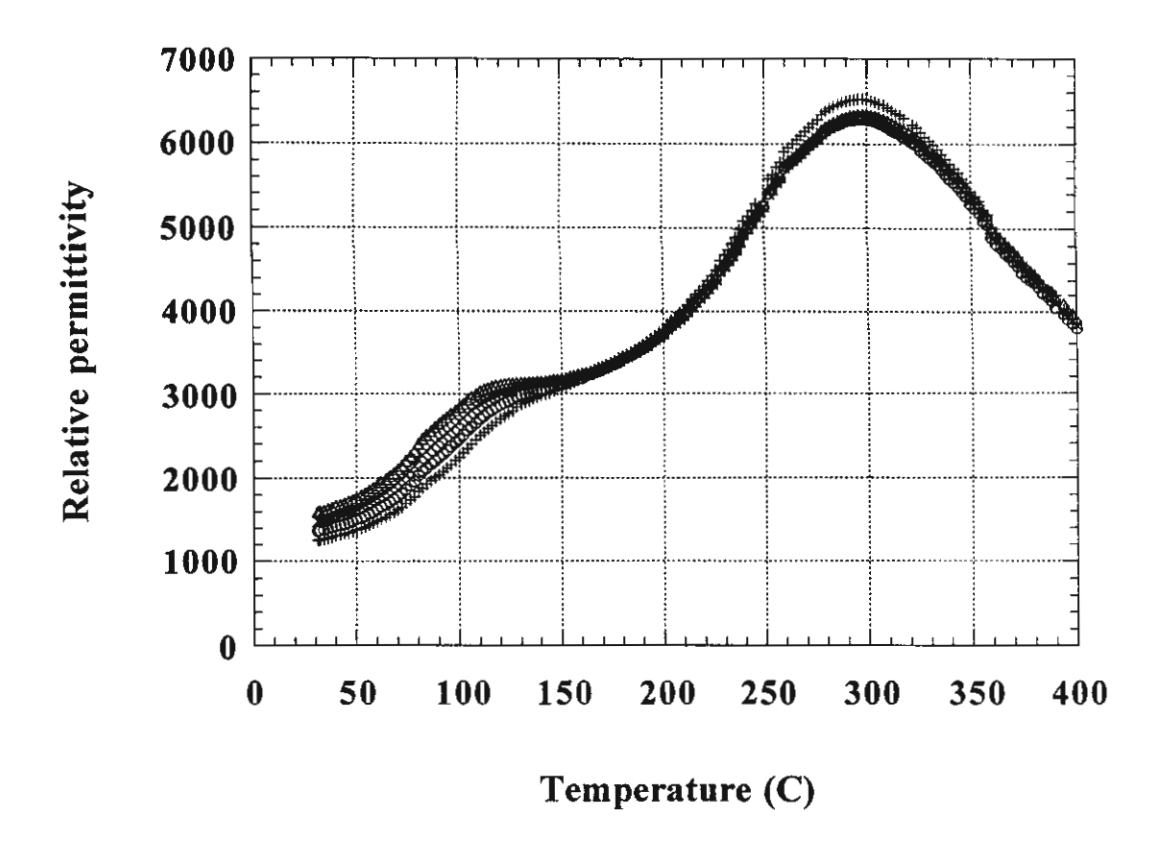


Figure 11 Change in relative permittivity and dissipation factor with temperature and frequency of 0.9(Bi_{0.45}La_{0.05}Na_{0.5}TiO₃)-0.1PT



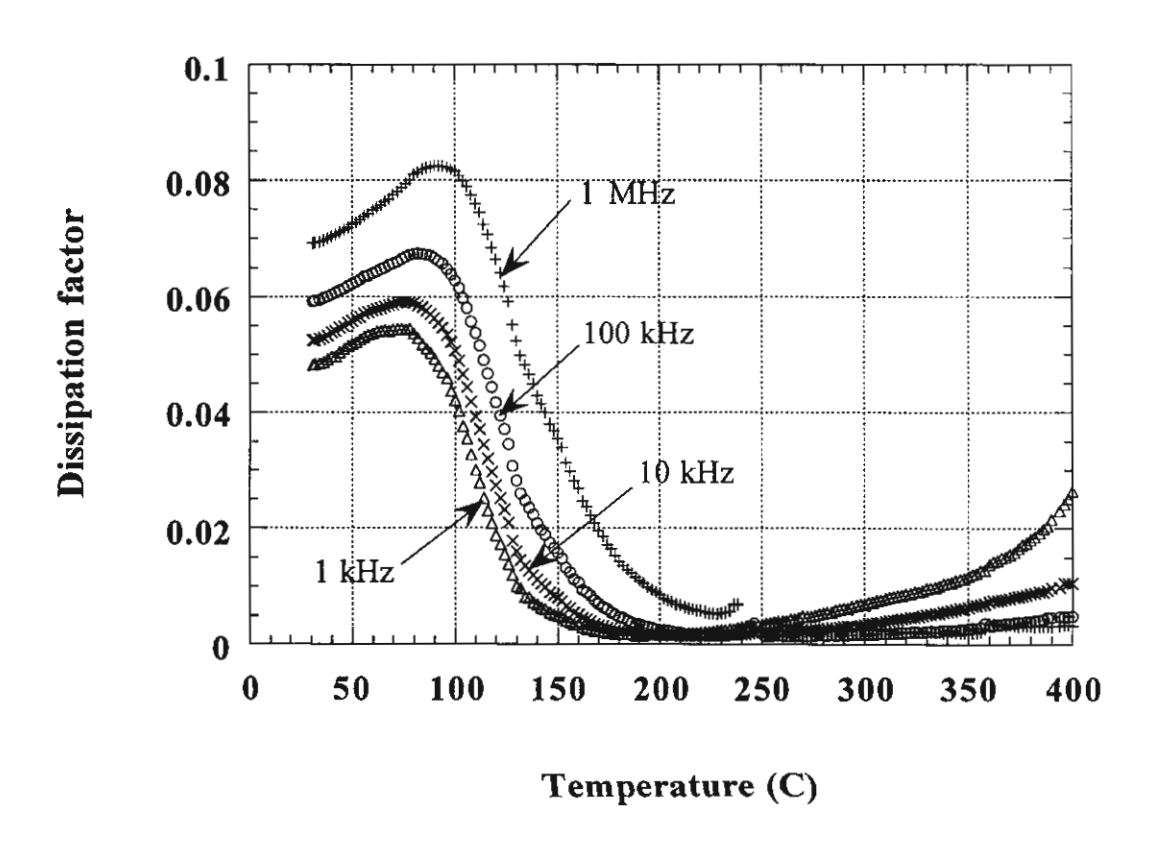
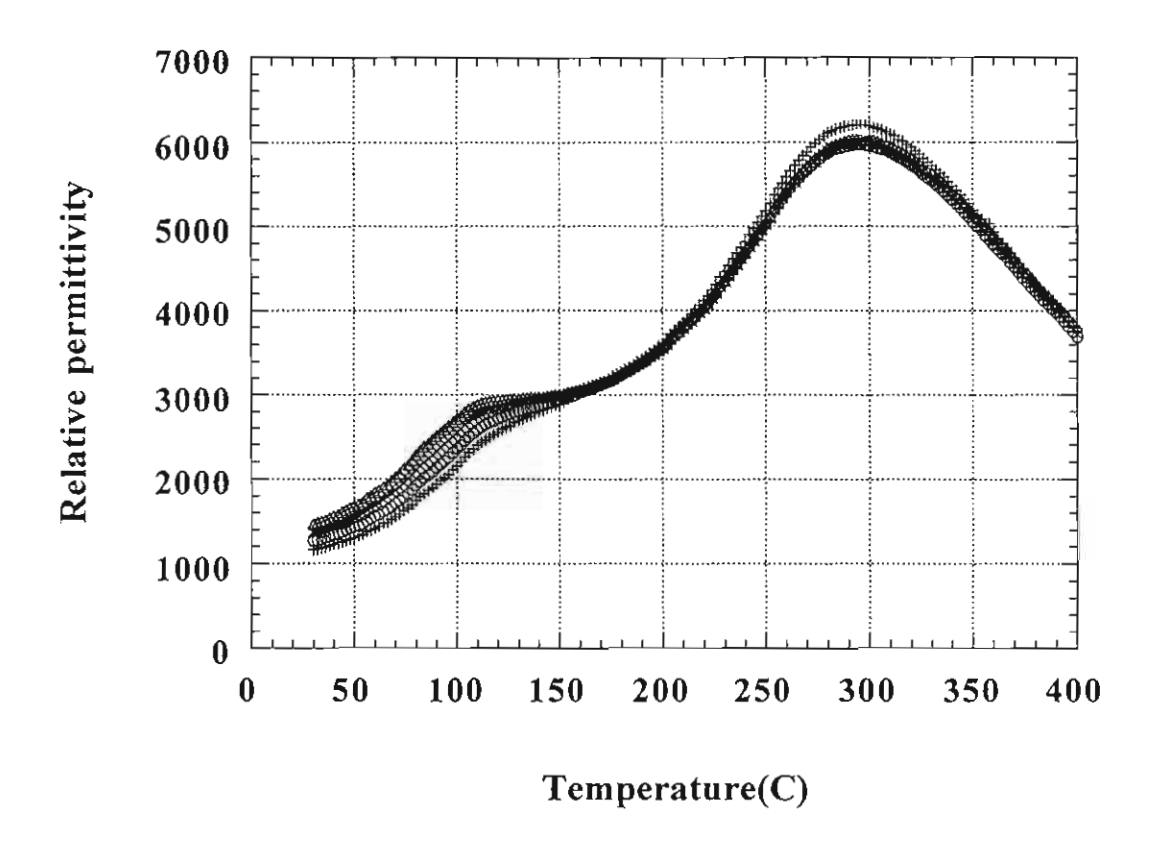


Figure 12 Change in relative permittivity and dissipation factor with temperature and frequency of 0.88(Bi_{0.48}La_{0.02}Na_{0.5}TiO₃)-0.12PT



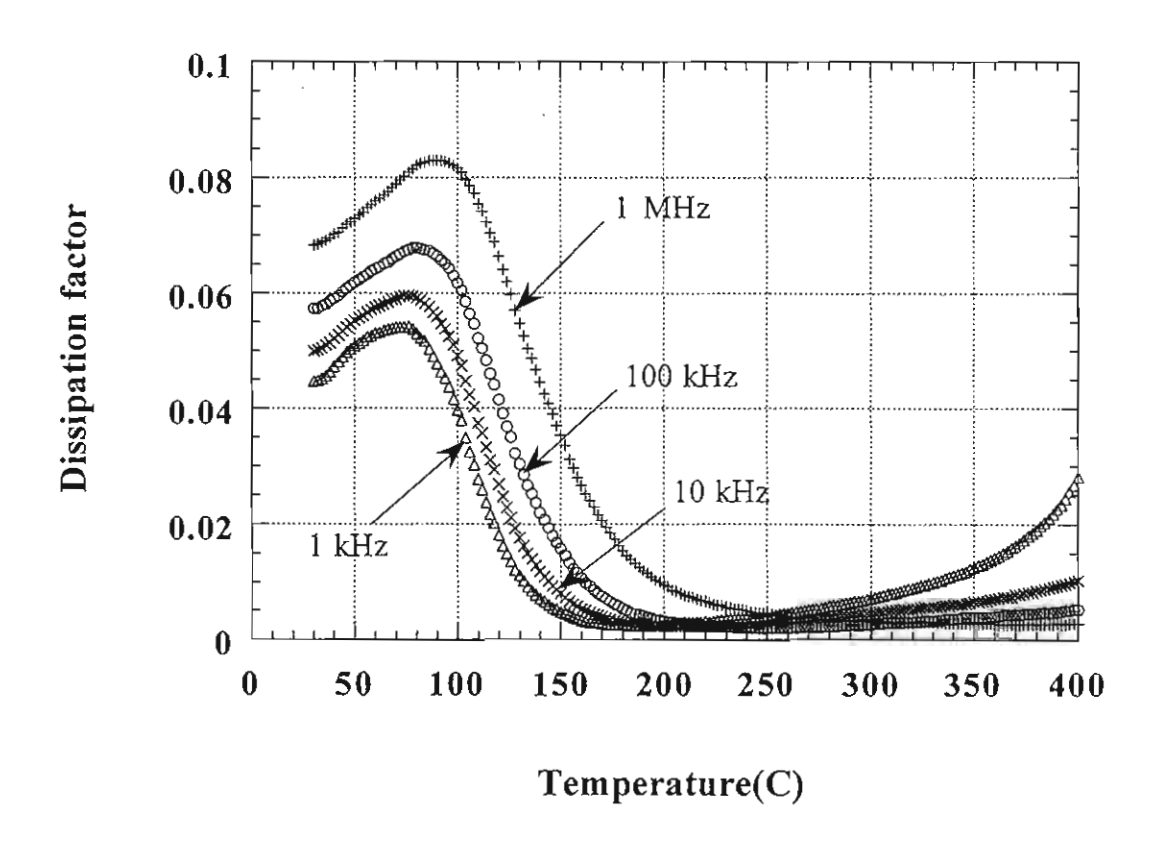
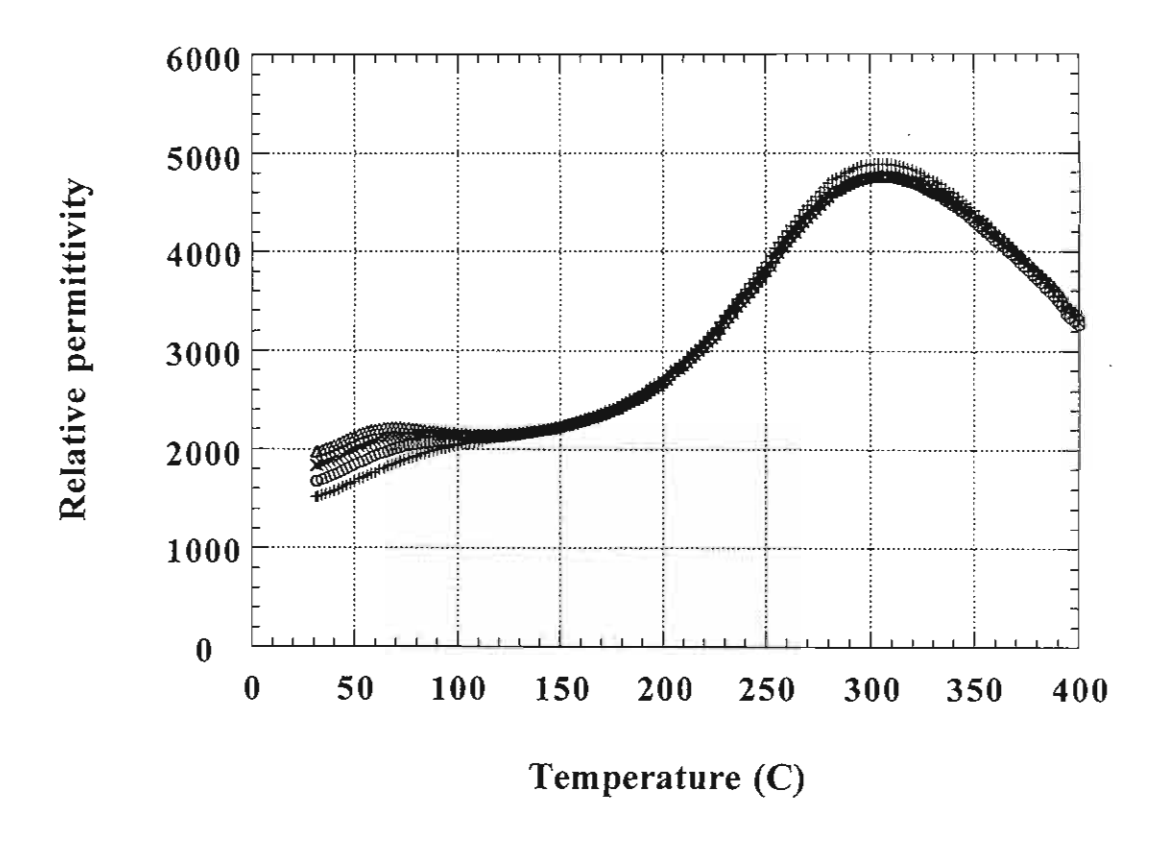


Figure 13 Change in relative permittivity and dissipation factor with temperature and frequency of 0.9(Bi_{0.48}La_{0.02}Na_{0.48}K_{0.02}TiO₃)-0.1PT



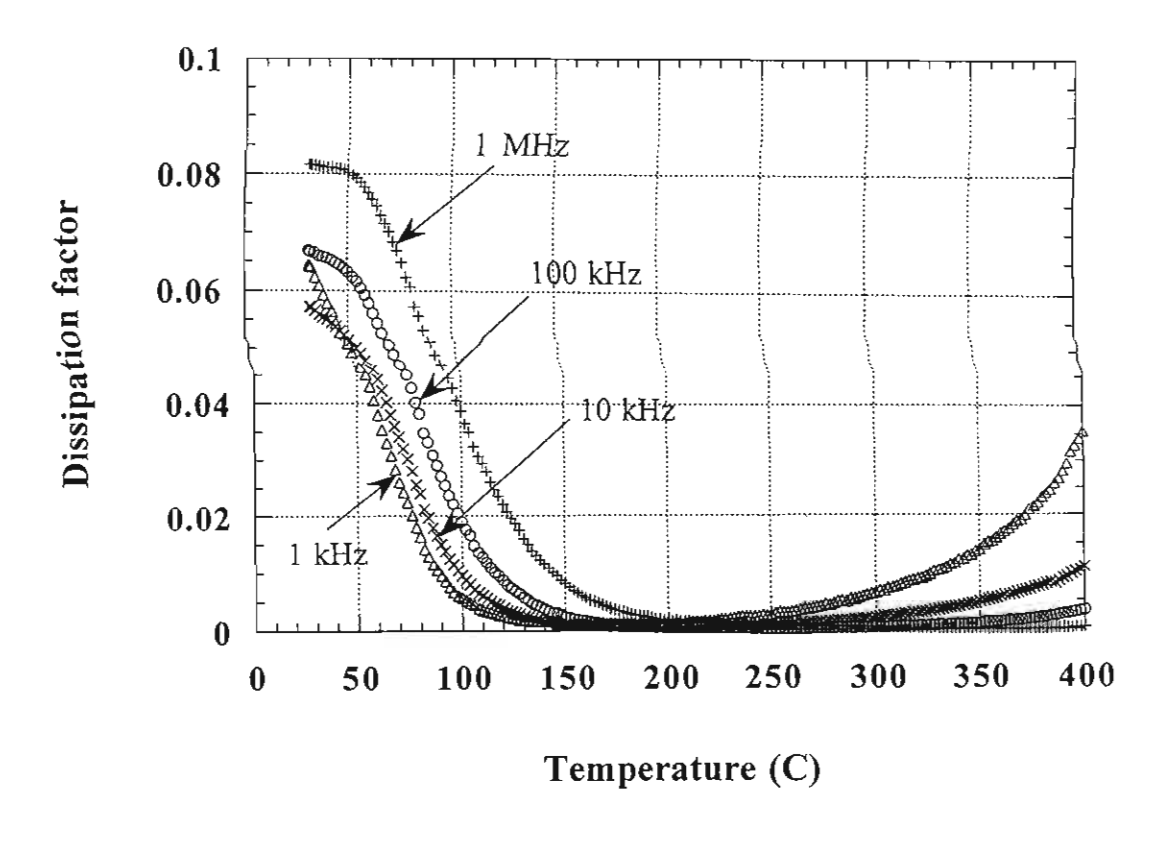
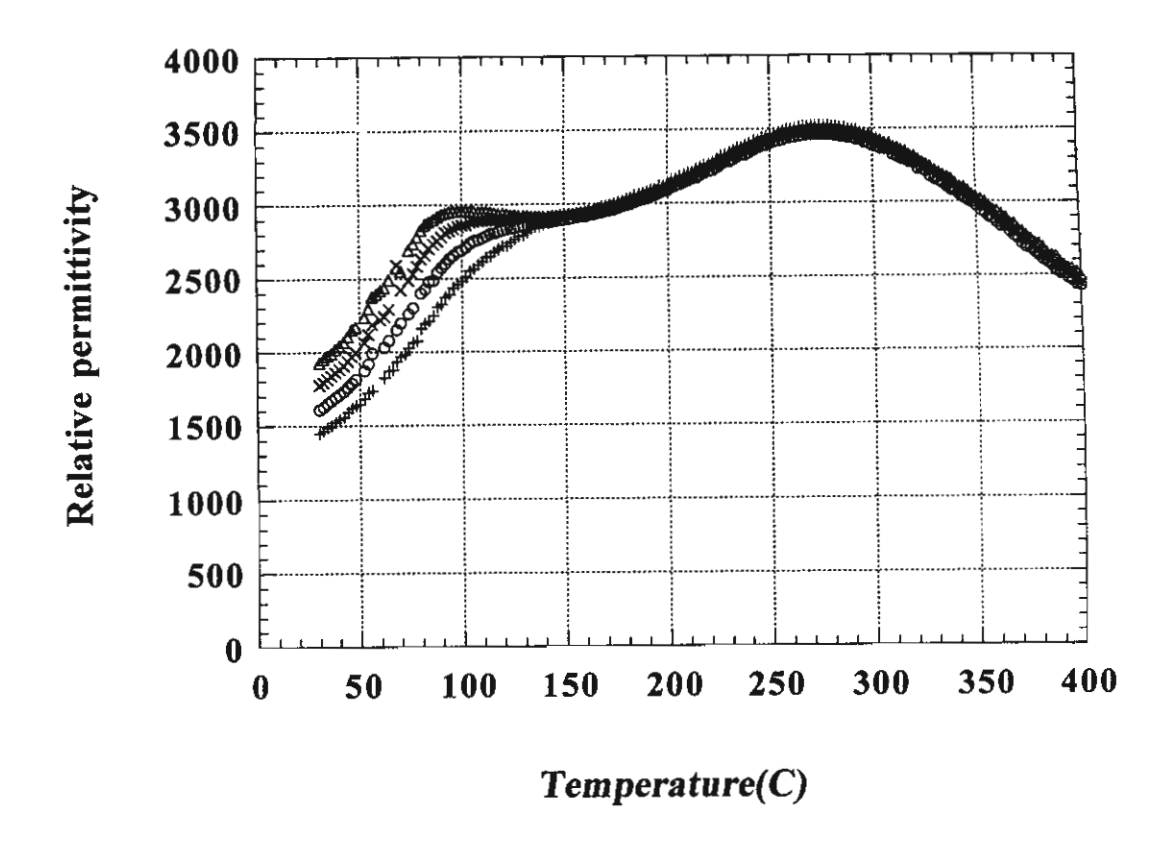


Figure 14 Change in relative permittivity and dissipation factor with temperature and frequency of 0.9(Bi_{0.48}La_{0.02}Na_{0.46}K_{0.04}TiO₃)-0.1PT



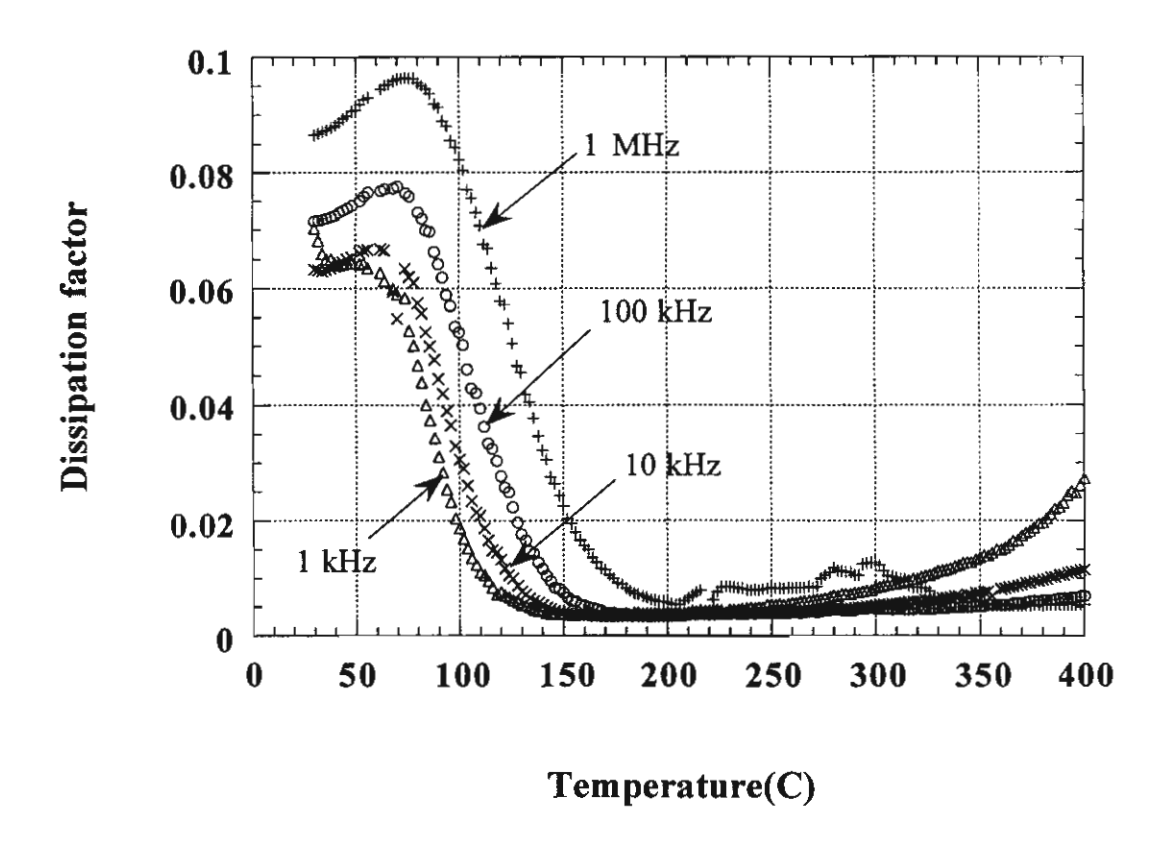
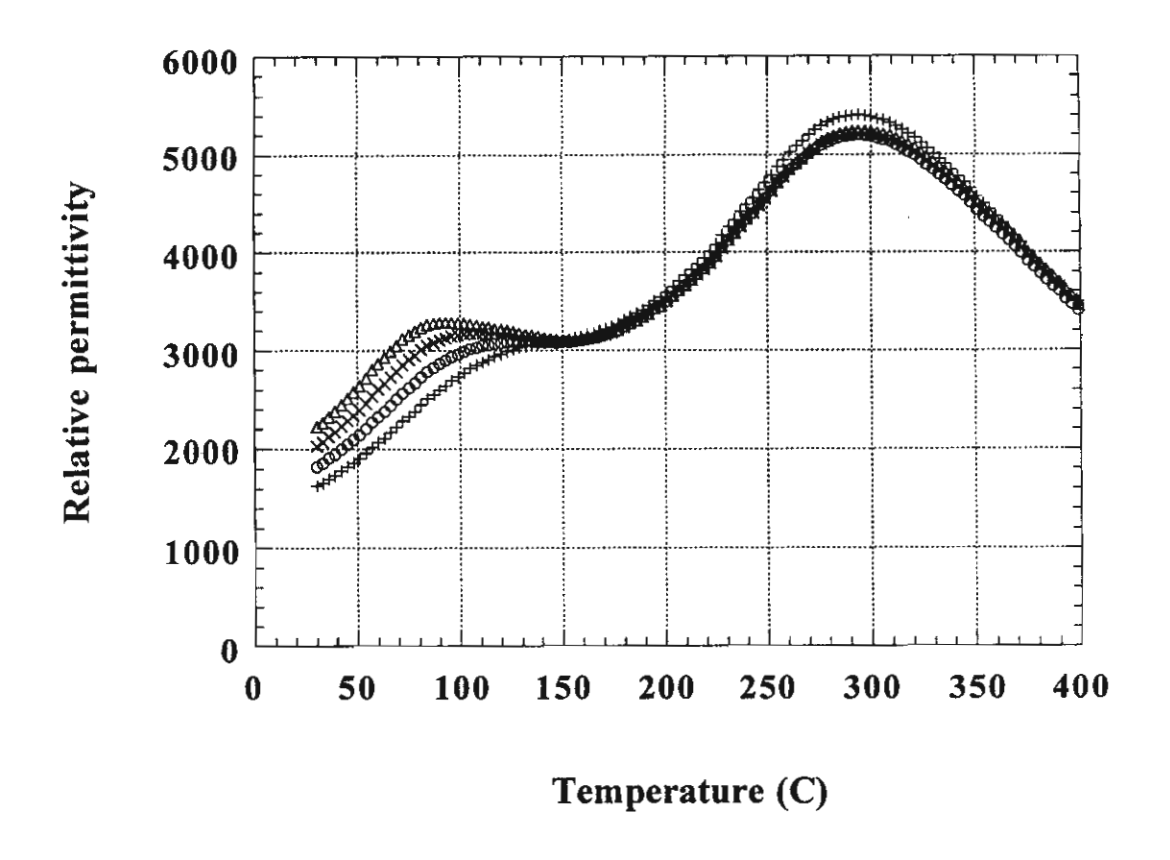


Figure 15 Change in relative permittivity and dissipation factor with temperature and frequency of 5%Nb-doped BNT-10PT



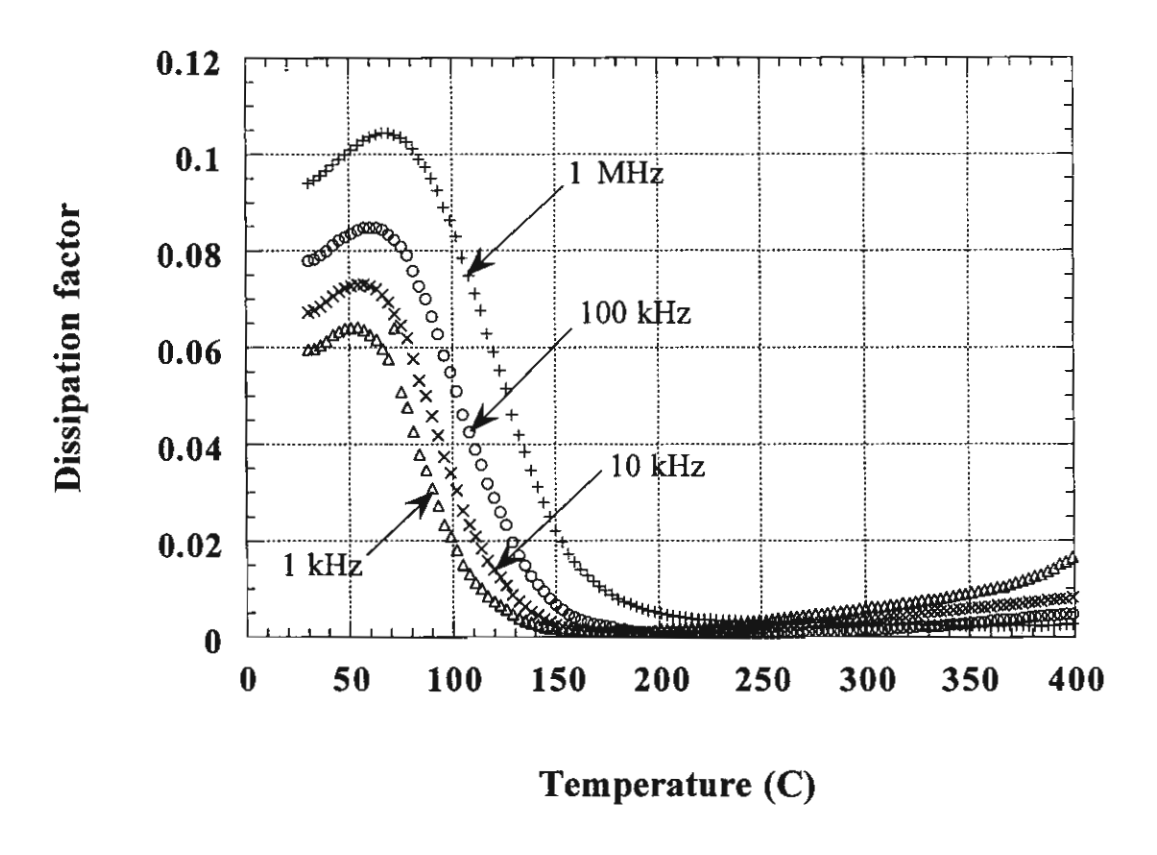
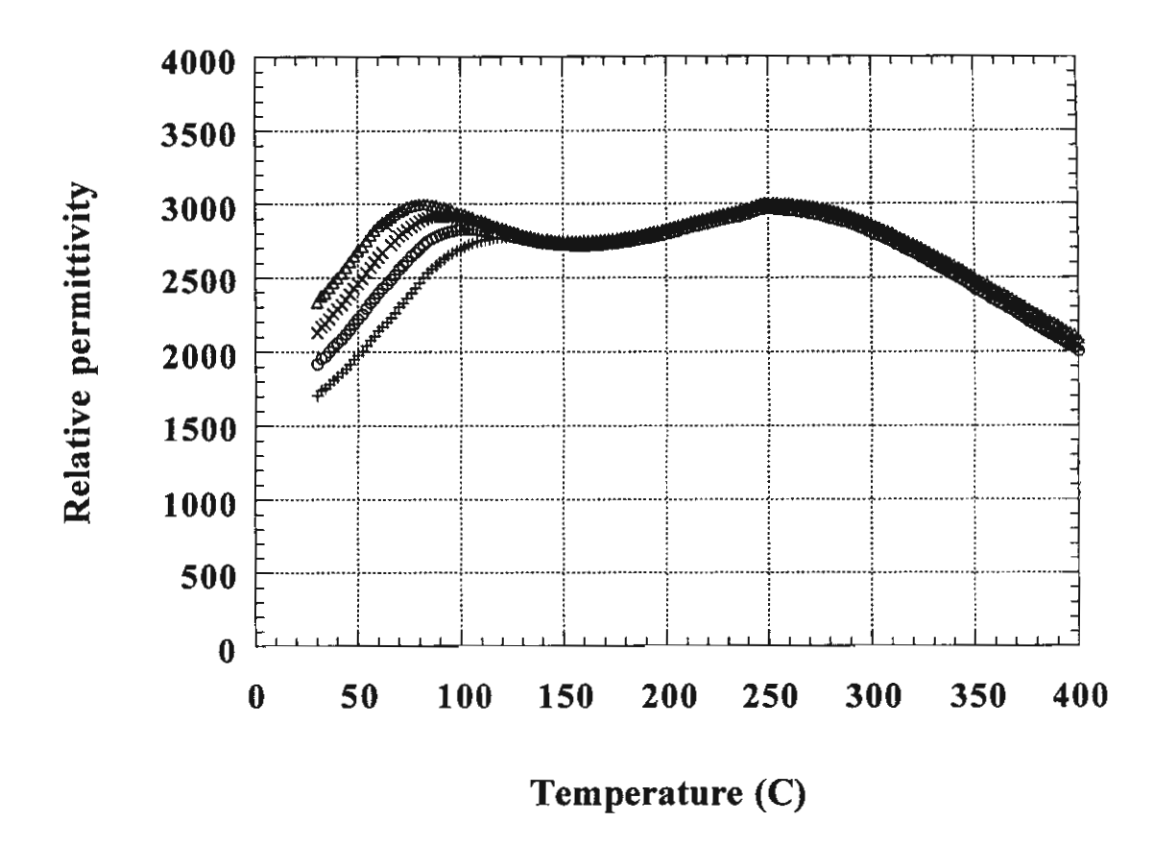


Figure 16 Change in relative permittivity and dissipation factor with temperature and frequency of 5%Nb-doped BNT-15PT



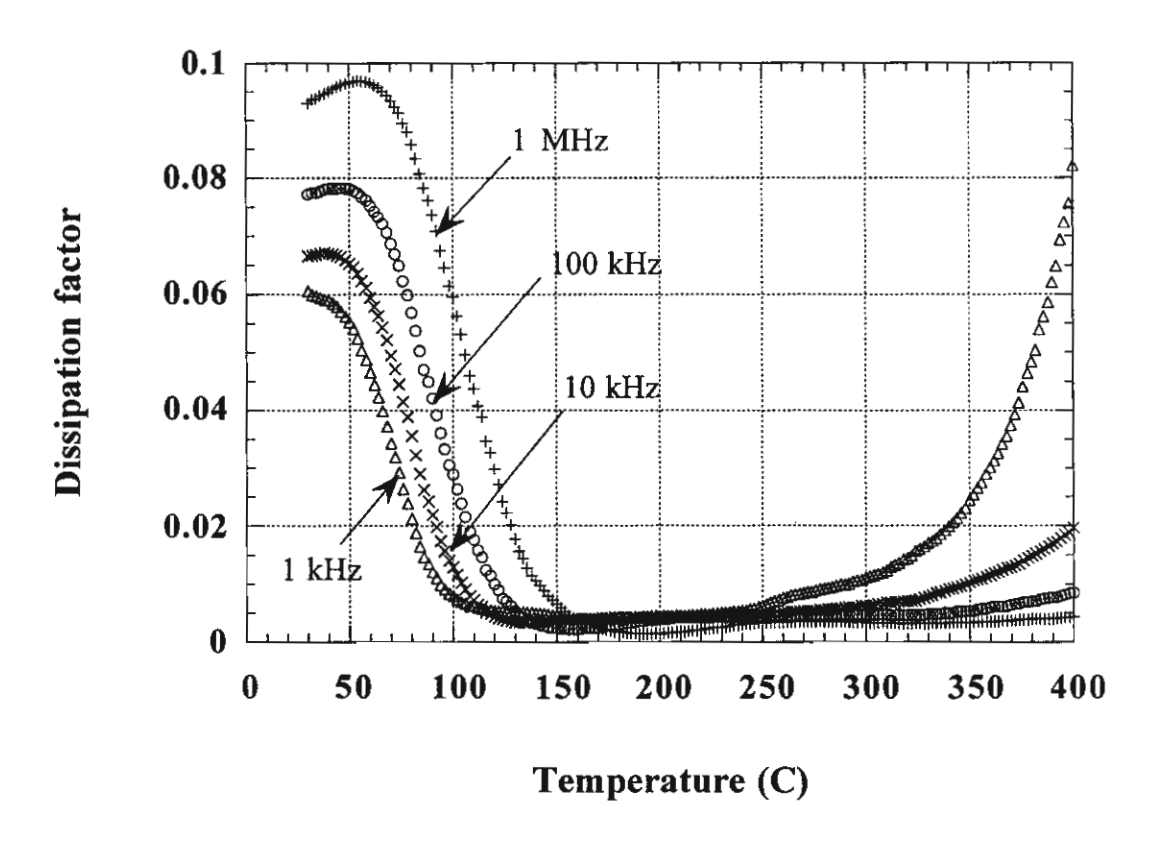
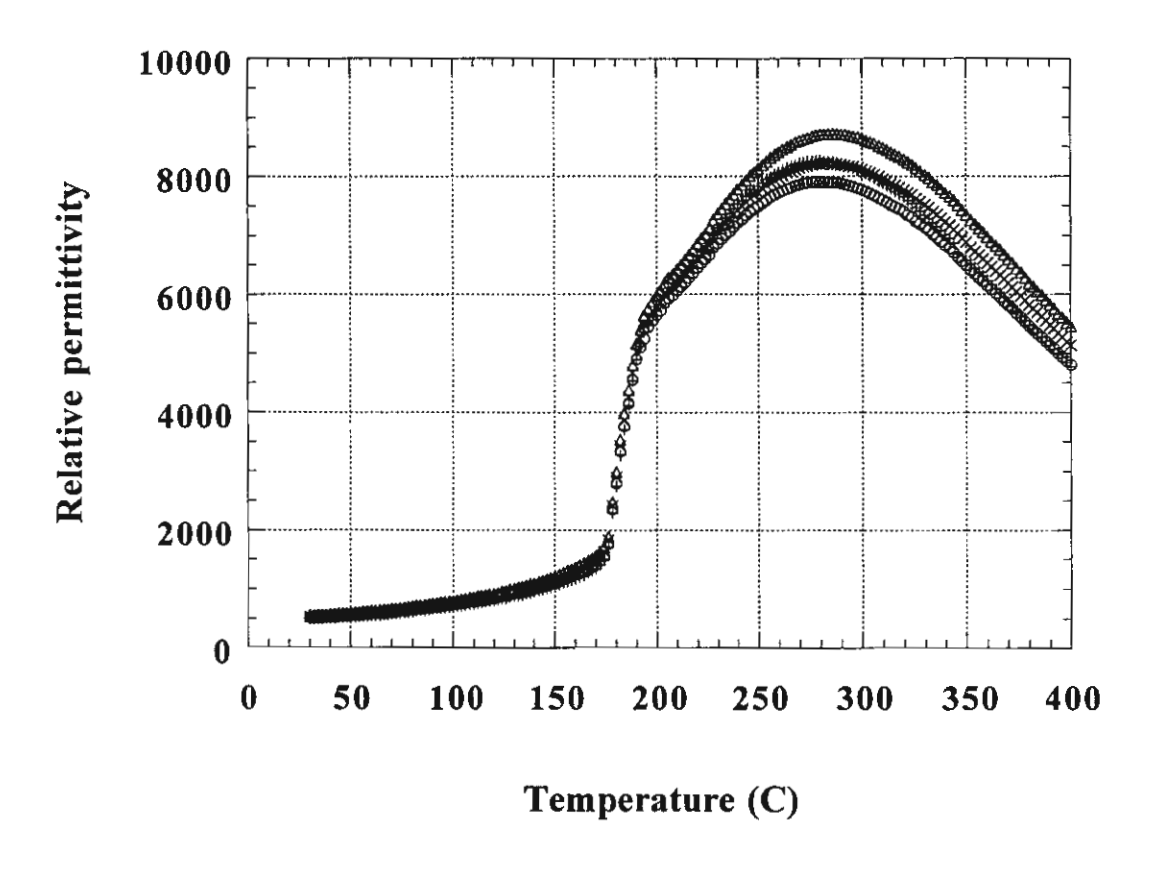


Figure 17 Change in relative permittivity and dissipation factor with temperature and frequency of 10%Nb-doped BNT-10PT



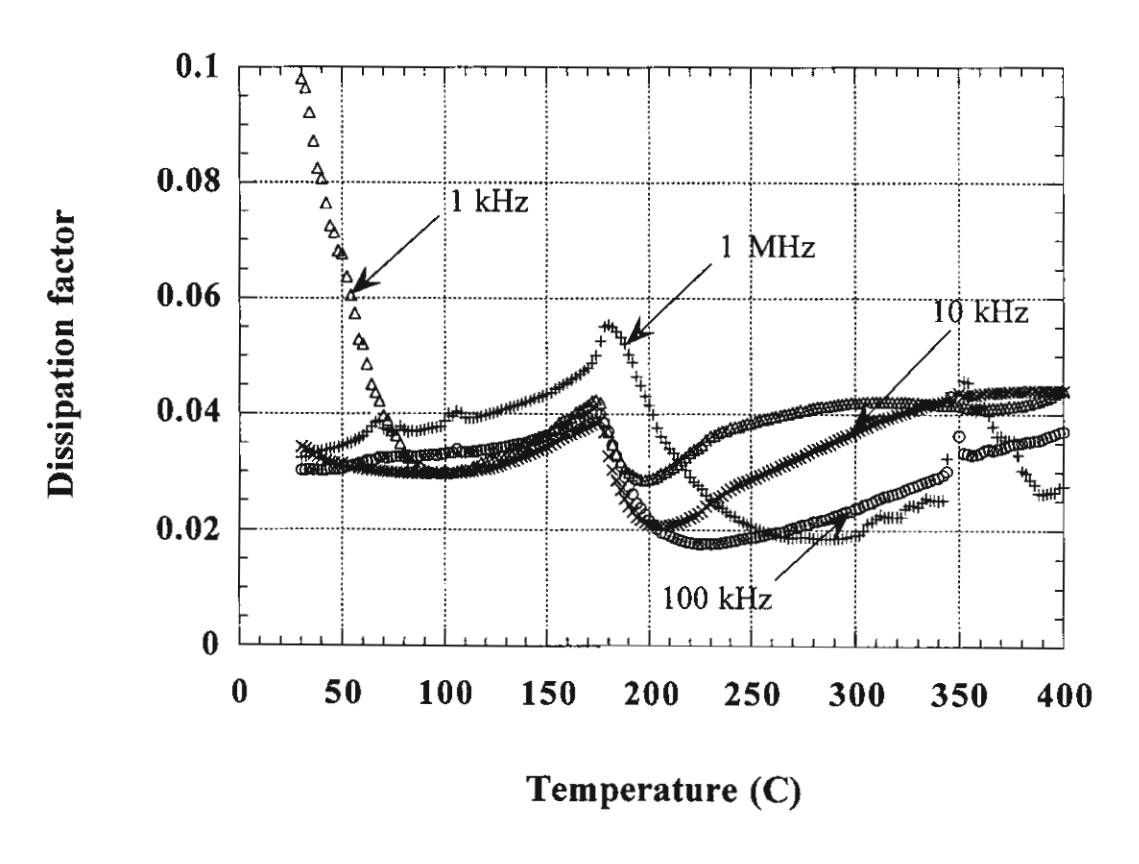


Figure 18 Change in relative permittivity and dissipation factor with temperature and frequency of 0.9BNT-0.1PbTi_{0.9}Mn_{0.1}O₃

Table 3 Maximum K', the first and second transition temperatures as a function of frequency and composition

$0.9(Bi_{0.45}La_{0.05}Na_{0.5}TiO_3)-0.1PbTiO_3$

Frequency (kHz)	Maximum K'	Tt1(°C)	Tt2(°C)
1	3664	110	288
10	3645	112	288
100	3640	117_	286
1000	3710	121	288

$0.88(Bi_{0.48}La_{0.02}Na_{0.5}TiO_3)-0.12PbTiO_3$

Frequency (kHz)	Maximum K'	Tt1(°C)	Tt2(°C)
1	6343	112	298
10	6300	116	298
100	6284	120	298
1000	6520	126	298

$0.9 (Bi_{0.48} La_{0.02} Na_{0.48} K_{0.02} TiO_3) - 0.1 PbTiO_3$

Frequency (kHz)	Maximum K'	Tt1(°C)	Tt2(°C)
11	6035	110	296
10	5990	112	294
100	5964	117	294
1000	6200	121	294

$0.9(Bi_{0.48}La_{0.02}Na_{0.46}K_{0.04}TiO_3)-0.1PbTiO_3$

Frequency (kHz)	Maximum K'	Tt1(°C)	Tt2(°C)
1	4780	62	306
10	4756	67	306
100	4750	74	306
1000	4892	80	304